

RSC Advances



This is an *Accepted Manuscript*, which has been through the Royal Society of Chemistry peer review process and has been accepted for publication.

Accepted Manuscripts are published online shortly after acceptance, before technical editing, formatting and proof reading. Using this free service, authors can make their results available to the community, in citable form, before we publish the edited article. This *Accepted Manuscript* will be replaced by the edited, formatted and paginated article as soon as this is available.

You can find more information about *Accepted Manuscripts* in the [Information for Authors](#).

Please note that technical editing may introduce minor changes to the text and/or graphics, which may alter content. The journal's standard [Terms & Conditions](#) and the [Ethical guidelines](#) still apply. In no event shall the Royal Society of Chemistry be held responsible for any errors or omissions in this *Accepted Manuscript* or any consequences arising from the use of any information it contains.

Cite this: DOI: 10.1039/c0xx00000x

www.rsc.org/xxxxxx

PAPER

Dechlorination of hexachlorobenzene by nano zero-valent iron/activated carbon composite: iron loading, kinetics and pathway

Wei-fang Chen^{a*}, Ling Pan^a, Li-fang Chen^b, Qiong Wang^a, Chang-cheng Yan^a

Received (in XXX, XXX) Xth XXXXXXXXX 20XX, Accepted Xth XXXXXXXXX 20XX

DOI: 10.1039/b000000x

Abstract

Nano zero-valent iron (nZVI) and activated carbon composites were synthesized and employed to remove hexachlorobenzene (HCB). Methods of impregnation and adsorption were employed to load iron salt onto activated carbon first and thus loaded iron was then reduced to form zero valent iron. Results indicate that method of iron loading greatly impacted the amount of iron and HCB dechlorination. In general, nZVI/activated carbon composite synthesized using an adsorption method showed much higher removal efficiency and dechlorination capability. More than 80% of the HCB was dechlorinated after 48 h. Dechlorination of HCB followed a stepwise pathway: HCB (hexachlorobenzene)→PCB (pentachlorobenzene)→1,2,4,5TeCB (tetrachlorobenzene)→TriCB (trichlorobenzene)→1,4 DCB (dichlorobenzene)→MCB (monochlorobenzene). Compared with activated carbon or nZVI, nZVI/activated carbon composite showed much higher HCB removal. Analysis of mass partition on solid and aqueous phases indicates that most of the HCB and its dechlorination intermediates were retained on solids probably due to activated carbon's strong adsorption. In summary, activated carbon's function is 3 folds: it alleviated the problem of nZVI agglomeration, contributed to HCB removal by its own adsorption capability and increased the nZVI's resistance against pH change.

Keywords: nano zero-valent iron; activated carbon; hexachlorobenzene; dechlorination

1. Introduction

Once considered an effective fungicide, rubber peptizing agent and wood preservative etc., hexachlorobenzene (HCB) was now banned for commercial production in many countries [1]. However, HCB still contaminates many sites and streams in China due to its persistence in the environment. Studies have related HCB to cases of breast cancer and various organ damages [2]. Together with other members from the halogenated organic compounds family, efficient and cost-effective remediation methods are required to treat locations with HCB pollution.

Zero-valent iron was found to be an effective dehalogenation reagent due to its reducing power [3]. In particular, studies have

shown that nano zero-valent iron (nZVI) could provide even more rapid and complete reduction of halogenated hydrocarbon [4]. As a result, the use of nZVI for in situ remediation of organic and inorganic pollution in soil and groundwater had gained much momentum over the last decade [5]. Application of pure nZVI, however, was limited by the material's strong tendency to agglomerate, low wettability with organic phase and high density difference to water. All these characteristics contributed to the low mobility and loss of reactivity of nZVI in aqueous stream [6]. Many studies employed additives (e.g. anionic polyelectrolyte, surfactant etc.) to improve mobility and create stable nZVI suspension [7]. Besides additives, depositing nZVI on carrier materials has been explored extensively as another way to

overcome nZVI's limitations and extend its environmental applicability. Silica [8], alginate bead [9], carbon black [10], zeolite [11], carbon nanotube [12], activated carbon [13] are among the various material investigated as carriers.

In this study, activated carbon was chosen as the carrying material. Activated carbon is renowned for its high surface area and pore volume. The pore structure of activated provides ample rooms for nZVI. Bleyl argued that activated carbon's pore system provided a foundation for the formation of finely dispersed nano-iron cluster [14]. Also, activated carbon is very effective for adsorption of organics, which creates an environment of enriched organics around nZVI particles, thus may accelerate destruction of pollutants. This is especially beneficial in the environment where concentration of pollutant is low as often in the case of a groundwater plume. Xu et al. believed that sorption-assisted dechlorination greatly sped up the destruction of pollutant in their study of 2,4-dichlorophenol removal when Pb/Fe nano particles was dispersed on a multi-walled carbon nanotube support [12].

However, there are many ways to deposit nZVI on supporting materials. In general, production of ZVI-supported materials was divided into two steps. Fe (II) or Fe (III) was first adsorbed or impregnated onto material and then reduced to form nZVI. Chemical reduction by NaBH₄ of Fe (II) or Fe (III) on the carrier is among the most popular due to its simplicity in operation especially at lab-scale. For carbon-based carriers, there are also many reports of carbothermal synthesis of nZVI-carbon composite using the reductive power of carbon element [15, 16]. Tseng et al. combined chemical reduction with high temperature calcinations (700°C) in N₂ atmosphere for their synthesis of activated carbon/zero valent iron composite for the purpose of TCE removal [17]. Their results showed that calcination helped to further disperse ZVI particles in activated carbon and a higher TCE removal was achieved.

This study undertook to assess the effectiveness of HCB removal by activated carbon supported nZVI. Effect of dosage and pH, HCB removal kinetics, and dechlorination pathway were investigated. Chemical reduction by NaBH₄ was employed to reduce iron salt to zero valent iron. The effects of iron loading by wet impregnation and adsorption on morphology of synthesized nZVI and effects on HCB dechlorination were also studied.

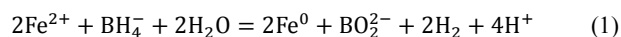
2. Materials and methods

2.1 Chemicals

Lignite-based granular activated carbon, sodium borohydride, ethanol and n-hexane were purchased from Sinopharm Chemical (Shanghai, China). Hexachlorobenzene, ferrous chloride tetrahydrate and chlorobenzene standard solutions were obtained from Aladdin Industrial Co., (Shanghai, China). All chemicals were of analytical grade and used as received. All the reagents were prepared with deionized water.

2.2 Preparation of nZVI/activated carbon

Activated carbons of 88-150 μm in size were used as the nZVI carrier. There were two steps in making the nZVI/activated carbon composite. First, ferrous salts were loaded onto activated carbon by wet impregnation or adsorption process. Loaded iron was then reduced to Fe⁰ by NaBH₄ according to the following reaction (1) [18]:



In wet impregnation, 2 g of activated carbon was added to 50 mL of ferrous chloride solution (concentration of 1 mol/L). The resulting slurry was shaken for 24 h on a rotary shaker at room

temperature (25°C) and then put in an evaporator at 100 °C for 5 h. For nZVI/activated carbon composite synthesis, 2 g of iron-impregnated activated carbon was added slowly to 50 mL of 1 mol/L NaBH₄. After 3 h of reaction, nZVI/activated carbon was separated by filtration from liquid and washed thoroughly with deionized water to get rid of loose nZVI, dried and stored in N₂ purged container. Thus synthesized nZVI/activated carbon was named as nZVI/AC-I.

In adsorption, 2 g of activated carbon was added to 20 mL of 1 mol/L of ferrous chloride solution. The mixture was shaken for 24 h on a rotary shaker at 25°C. 15 mL of ethanol and 15 mL of water were then added to the mixture. After that, 50 mL of 1 mol/L NaBH₄ was added to the mixture dropwise and with vigorous stirring. The resulted particles were separated and named as nZVI/AC-A.

For comparison, nZVI was synthesized using the modified NaBH₄ reduction method [19]. 21.36 g of ferrous chloride was added to a mixture of 96 mL of ethanol and 24 mL of water. The solution was added slowly to 400 mL of 1 mol/L NaBH₄ and then was shaken for 2 h on a rotary shaker at 25°C. After that, particles were separated, washed, dried and stored in N₂ purged container.

2.3 Characterization of nZVI/AC

Surface area and pore size distribution were determined by nitrogen adsorption-desorption isotherms at a temperature of 77 K (-196°C) by a 3H-2000PS4 unit (Beishide Instrument, China). Total pore volume was estimated from the adsorbed amount at a relative pressure of 0.99. Brunauer-Emmett-Teller (BET) and Barrett-Joyner-Halenda (BJH) equations were used to calculate surface area and pore size distribution respectively.

Scanning Electron Microscope (SEM) S4800 (Hitachi, Japan) and High Resolution Transmission Electron Microscope (HR-

TEM) Tecnai G20 (FEI, USA) were used to observe the morphology and size of the composites. Infrared spectra of the nZVI, nZVI/activated carbon were obtained by a Fourier Transform Infrared Spectrometer (FTIR) Magna-IR 750 (Nicolet, USA) in the diffuse reflectance mode with KBr pellets. Spectra were generated from the mid-infrared range from 4000-500 cm⁻¹ with 256 scans per spectrum at a spectral resolution of 4 cm⁻¹.

2.4 Effect of dosage on HCB removal

10, 30, 50, 80, 160 and 300 mg of nZVI, activated carbon or nZVI/AC composite was added to vials each containing 20 mL of 200 µg/L HCB solution. Initial pH was adjusted to 5.6. The mixtures were shaken for 8 h at 150 rpm and 25°C. Solid particles were separated from liquid by filtration. 0.45 µm membrane filter was used in all filtrations. Preliminary test indicates the membrane's retention of organics is negligible. Filtrate was extracted for 0.5 h with 20 mL of n-hexane and analyzed for HCB.

2.5 Effect of pH on HCB removal

nZVI, activated carbon or nZVI/AC, 160 mg in mass, was added to 20 mL of 200 µg/L HCB solution. pH of the solution was adjusted to 3, 5, 7, 9 and 11 using 0.5 mol/L HCl or NaOH. The mixtures were then shaken for 8 h at 150 rpm, 25°C. Solids were separated from liquid through filtration and filtrate extracted for HCB analysis.

2.6 HCB removal kinetics

nZVI, activated carbon or nZVI/activate carbon, 160 mg in mass, was added to 20 mL of 200 µg/L HCB solution. Initial pH of

solution was adjusted to 5.6. The mixtures were shaken for 0.5, 1, 4, 8, 24 and 48 h. At the end of each time interval, solids were separated from liquid by filtration. 10 mL of filtrate was extracted with 20 mL of n-hexane for 0.5 h to separate residual HCB or dechlorination products from water.

On the other hand, to determine the mass of organics retained by nZVI/AC-I or nZVI/AC-A solids, nZVI/AC-I or nZVI/AC-A was each mixed with 20 mL of n-hexane for 4 h to extract the adsorbed organics. HCB and its potential dechlorination products in the extract were analyzed.

All tests above were conducted in triplet.

2.7 Chemical analysis

HCB and its degradation chlorobenzene products were analyzed with an Agilent 7890A-5975C gas chromatography-mass spectrometry (Agilent Technologies, USA) equipped with an HP-5MS capillary column. 1 μ L of extraction was injected automatically in splitless mode. The temperatures of injector and detector were set at 320°C and 350°C respectively. Separation was controlled with a temperature program that started at oven temperature at 40°C, held for 5 min, then ramped at 20°C/min to 200°C, and then ramped at 5°C/min to 250°C, held for 2 min.

Iron content of activated carbon or nZVI/AC composite was determined by a digestion method. 0.1 g of sample was added to 30 mL of 3 mol/L HCl. The mixture was shaken for 2 h and the digestion solution was diluted and analyzed for iron by an AA-6300C Atomic Absorption Spectrophotometer unit (Purkinje General, China) with flame atomization.

3. Results and discussion

3.1 Characterization of nZVI/AC

Fig.1 (a)-(f) are illustrations of SEM and TEM images of activated carbon, nZVI, nZVI/AC-I and nZVI/AC-A. Activated carbon shows an uneven and porous surface. nZVI without support agglomerated severely into clusters (1(b)). nZVI was much more dispersed when activated carbon was used as a supporting material. However, the structure of nZVI differed with different iron loading method. As shown in Figure 1(c), with wet impregnation, the resultant nZVI was more randomly shaped. By comparison, with adsorption, nZVI was generally in a rod-like structure.

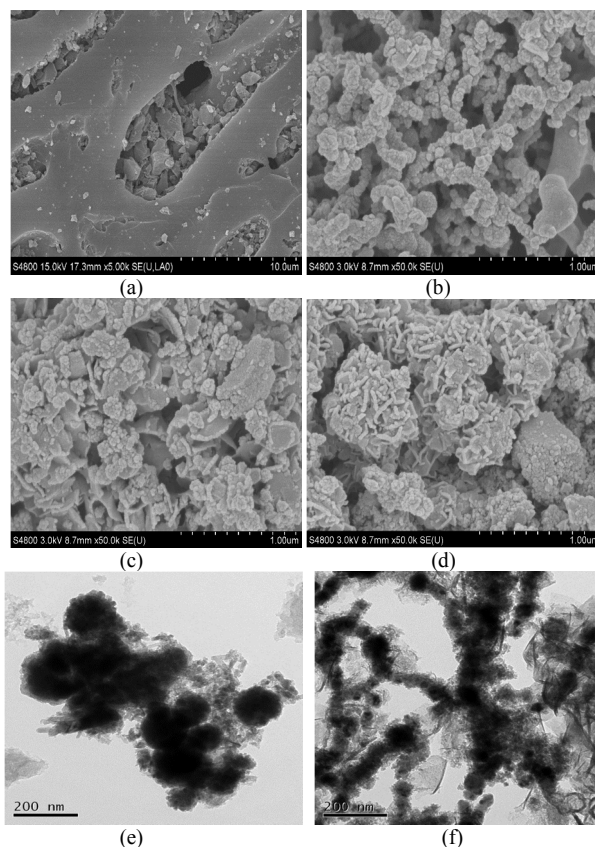


Fig.1 SEM images (magnitude 50.0 k) of (a) activated carbon (b) nZVI (c) nZVI/AC-I (d) nZVI/AC-A; TEM images of (e) nZVI/AC-I, (f) nZVI/AC-A

TEM images correspond well with images from SEM. The dark clusters in these images are identified to be iron particles. Fig.1(e) reveals that nZVI/AC-I composite consists of roughly spherical iron particles while those of nZVI/AC-A were more in rod shape. And particles from nZVI/AC-I are about 50 nm in diameter. Adsorption produced relatively smaller particles with diameter around 20 nm. The difference in size may be due to the difference in the morphology of loaded iron. In impregnation, water was evaporated, iron salts solidified and precipitated as iron (hydr)oxides and was later reduced. While in adsorption, iron was most likely adsorbed as hydrated or complexed ions. Ethanol could also be playing a role in limiting the size. Jiu et al. believed that the presence of ethanol could first increase the amount of iron loading [20]. Ferrous ions were bound to the hydroxyl groups in ethanol while the non-polar part of the ethanol could more easily attach to the non-polar surface of the activated carbon. Besides, ethanol formed a finite structure surrounding iron ions and the size of nanoparticles created is thus more limited.

The FTIR spectrum images of activated carbon, nZVI, nZVI/AC-I and nZVI/AC-A provide further confirmation of nZVI loading onto activated carbon. As shown in Fig.2, broad bands at around 3400 cm^{-1} in activated carbon and nZVI/AC composites were attributed to O-H stretching, most likely due to H_2O or C-OH [21]. Other characteristic bands include C=C at 1600 cm^{-1} , C-OH at 1130 cm^{-1} [22]. The strong vibration at 1355 cm^{-1} and 1100 cm^{-1} for nZVI/AC-A was probably due to hydroxyl groups stretching caused by ethanol used during sample preparation. Bands around 2000 cm^{-1} and at less than 900 cm^{-1} observed in nZVI, nZVI/AC-I and nZVI/AC-A were attributed in part to iron oxides. These bands were weaker with nZVI/AC-I and nZVI/AC-A indicating that less oxidation occurred for activated carbon-supported Fe^0 [23].

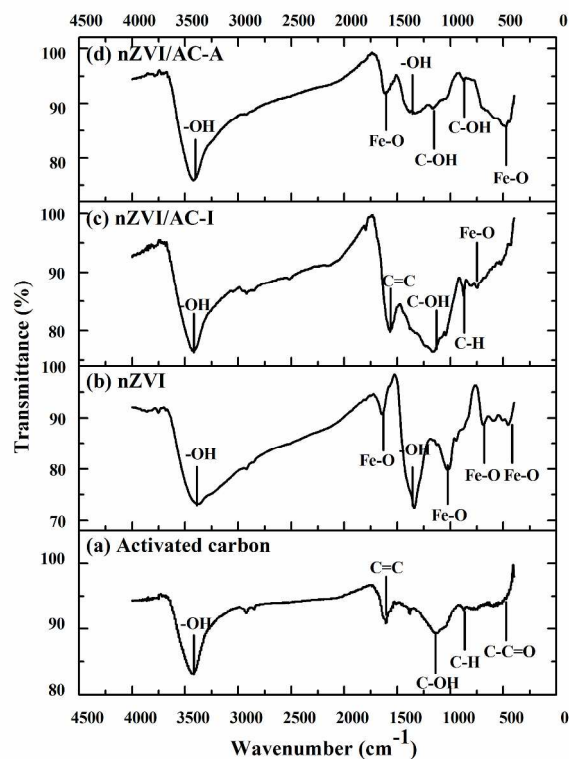


Fig.2 FTIR spectra of (a) activated carbon (b) nZVI (c) nZVI/AC-I (d) nZVI/AC-A

35

Fig.3 is the incremental pore volume vs. pore width for activated carbon, nZVI/AC-I and nZVI/AC-A. Table 1 lists the BET surface area and total pore volume. There are obvious drops in both surface area and pore volume after activated carbon was loaded with nZVI. This was mainly attributed to the fact that pores were occupied by nZVI. According to Fig.3, decrease in pore volume mostly occurred with pores less than 50 \AA in diameter indicating that those pores may be blocked by nZVI and no longer accessible.

45

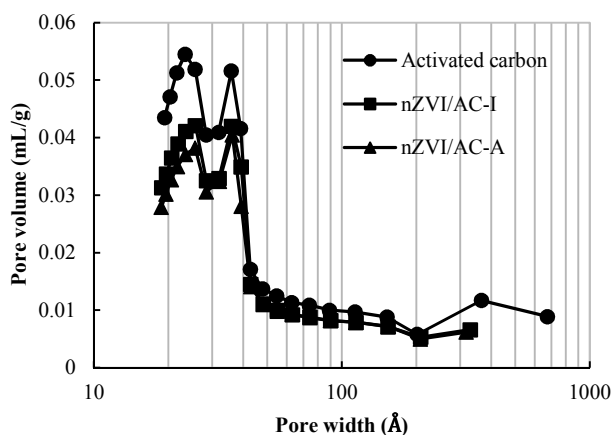


Fig.3 Pore size distribution of activated carbon, nZVI/AC-I and nZVI/AC-A

Table 1 is a summary of the surface area and total pore volume from pore size analysis. It also includes the iron contents for the samples. After synthesis, iron content increased from about 0.30 mg/g for activated carbon to 61.08 and 217.08 mg/g for nZVI/AC-I and nZVI/AC-A respectively.

Table 1 BET surface area, total pore volume and iron content of activated carbon, nZVI/AC-I and nZVI/AC-A

Samples	BET surface area (m ² /g)	Total pore volume (mL/g)	Iron content (mg/g)
Activated carbon	708±14	0.44±0.05	0.30±0.05
nZVI/AC-I	597±10	0.36±0.04	61.08±4.23
nZVI/AC-A	502±12	0.32±0.02	217.38±5.12

Through characterization, two nZVI/AC composites showed differences both in nZVI morphology and iron content. Iron loading process had significant effect on the amount of elemental iron and characteristics of nZVI thus created.

The difference in pollutant removal by these composites was next tested on HCB.

3.2 Effect of dosage on HCB removal

Fig.4 presents the effect of dosages of activated carbon, nZVI, nZVI/AC-I and nZVI/AC-A on HCB removal. In all cases, HCB removal increased with the increase of dosage until it started to level off after dosage reached 8 g/L. All other conditions being the same, there will be more reactive sites available for reaction at higher dosage, thus higher HCB removal. In addition, HCB varied with different material. For instance, at 8 g/L dosage, activated carbon, nZVI, nZVI/AC-I and nZVI/AC-A removed 61%, 40%, 85% and 95% of the initial HCB respectively. In general, at the same dosage, the removal efficiency followed the order of nZVI/AC-A>nZVI/AC-I>activated carbon>nZVI. It seems that combining nZVI with activated carbon showed a synergistic effect. nZVI/AC-A showed the highest HCB removal capability probably due to its high nZVI content. With more nZVI particles, there will be more surface sites for reactions.

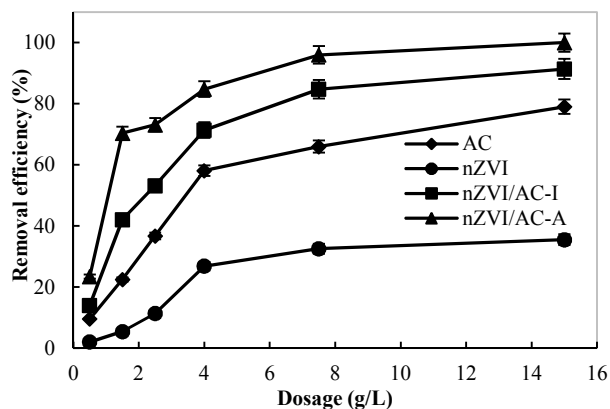


Fig.4 Effect of dosage on HCB removal by activated carbon, nZVI, nZVI/AC-I and nZVI/AC-A

3.3 Effect of initial pH

Fig.5 shows the effect of initial pH on HCB removal. Solution pH was adjusted to 2 to 11 before adding adsorbents. According to Fig.5, pH had significant effect only on HCB removal by nZVI. HCB removal was favorable at acidic pH. This may be because dissolution of the passivating (oxy)hydroxide layer on nZVI was

facilitated at low pH thus increased the reactivity. Also, at high pH (>9), Fe (II) and (III) hydroxides started to form and this could result in hydroxide covering the Fe⁰ surfaces and hampering electron transfer [24]. In contrast, statistical analysis (single factor t-test) revealed that variations in HCB removal by activated carbon, nZVI/AC-I and nZVI/AC-A were not significant at $\alpha=0.05$ level ($p\text{-value}>0.05$). Depositing of nZVI on activated carbon weakened the effect of pH and the materials were more robust against pH change. As for activated carbon, it removed HCB mainly by adsorption. Godino-Salido et al. believed that adsorption of aromatics on activated carbon consists of a plane to plane interaction between the aromatic moieties and the arene centres at the graphite sheets [25]. pH of solution may not have great effect on this mechanism.

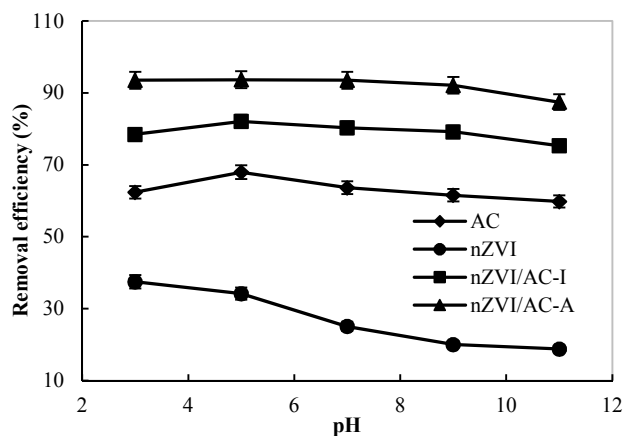


Fig.5 Effect of pH on HCB removal by activated carbon, nZVI, nZVI/AC-I and nZVI/AC-A

3.4 Adsorption kinetics

The effect of the reaction time on HCB removal is shown in Fig.6. For activated carbon, the removal efficiency increased from 26% at 0.5 h to around 45% at 8 h, then reached a plateau of around 65%. For nZVI/AC-I and nZVI/AC-A, the removal efficiency leveled off at 80% and 90% respectively after only 0.5 h of

contact. Removal by nZVI was much lower, it never reached beyond 30% even after 48 hours.

Kinetic data were fitted to pseudo-first and second order kinetic equations (2) and (3).

Pseudo-first order:

$$\log(q_e - q_t) = \log q_e - \frac{k_1}{2.303} t \quad (2)$$

Pseudo-second order:

$$\frac{1}{q_t} = \frac{1}{k_2 q_e^2} + \frac{1}{q_e} t \quad (3)$$

Where q_t and q_e are adsorption at time t and equilibrium. k_1 and k_2 are first and second order adsorption rate constants.

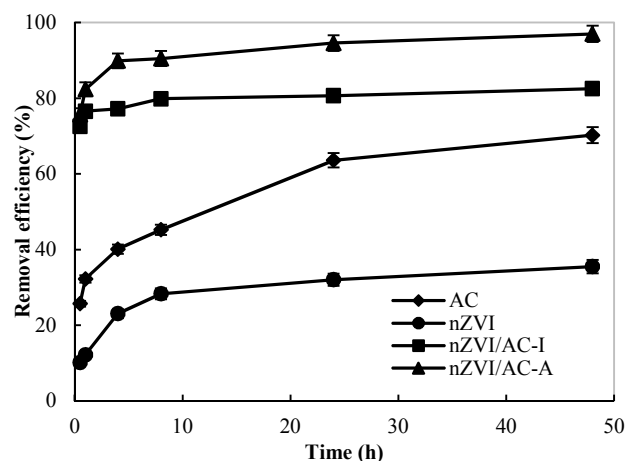


Fig.6 Effect of contact time on HCB removal by activated carbon, nZVI, nZVI/AC-I and nZVI/AC-A

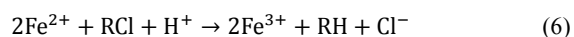
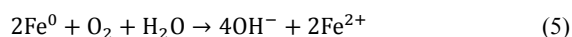
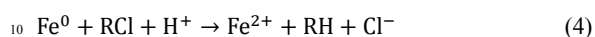
Table 2 lists the kinetic parameters of first and second order reactions. It is noted that, in all cases, correlation coefficient (R^2) for pseudo-first order model is less than 0.90 which is indicative of a bad correlation. The application of pseudo-second order model leads to much better coefficient of around 0.98-0.99. Moreover, the calculated values of q_e are in much better agreement with experimental data. Thus, second order kinetic model is more suitable to depict HCB removal suggesting that the process involves chemical reaction mechanism.

Table 2 Parameters for kinetics of HCB removal by activated carbon, nZVI, nZVI-I and nZVI-A

Samples	Pseudo-first order				Pseudo-second order			
	$q_{e,exp}^a$	$q_{e,cal}^b$	k_1	R^2	$q_{e,cal}^b$	k_2	R^2	$q_{e,exp}^1$
	(mg/g)	(mg/g)	(1/h)		(mg/g)	(g/(mg·h))		(mg/g)
Activated carbon	9.85	20.49	0.32	0.89	9.28	0.024	0.99	9.85
nZVI	7.98	4.57	0.08	0.88	8.13	0.057	0.99	7.98
nZVI/AC-I	18.34	1.52	0.06	0.77	18.34	0.25	0.99	18.34
nZVI/AC-A	21.55	3.27	0.08	0.86	21.59	0.13	0.98	21.55

^a experimental data ^bcalculated from model

Reactions of dechlorination and oxidation of zero-valent iron to Fe(II) or Fe(III) as follows (equations 4-8) could occur when nZVI came into contact with chlorinated organics [31].



nZVI/AC-A manifested the highest HCB removal capacity, with calculated adsorption capacity at equilibrium of 21.55 mg/g which is more than double that of activated carbon or nZVI. In addition, second order reaction rates (k_2) were one magnitude higher for nZVI/AC-I and nZVI/AC-A, indicating that the combination of activated carbon and nZVI also improved rates of removal.

Table 3 compares the HCB reactions rates reported in peer-reviewed journals to results obtained from this research. nZVI/AC-A manifested a relatively faster reduction than kaolin, activated carbon, nanoscale Fe, Pd/Fe or Cu/Fe particles and a slower reduction than Ag/Fe particles indicating that the materials synthesized could be quite competitive.

Table 3 Comparison of HCB reaction rates with other materials

Material description	Reaction rate constants	References
Kaolin	0.0047	[26]
Nanoscale Fe	0.14	[27]
Nanoscale Pd/Fe particles	0.23	[27]
Nanoscale Cu/Fe particles	0.056	[28]
Nano Ni/Fe particles	0.065	[29]
Micro Ag/Fe particles	0.452	[30]
Activated carbon	0.024	This research
nZVI/AC-I	0.13	This research
nZVI/AC-A	0.25	This research

In addition, concentration of iron in solution was monitored throughout the kinetics test. Overall, leaching of iron is not significant as iron concentration never reached beyond 0.08 mg/L in all situations. It appears that Fe(II) or Fe(III) produced during the dechlorination process was retained by activated carbon and there is little leaching of iron.

3.5 Pathway of HCB dechlorination reaction

Since dechlorination reactions may occur during HCB removal especially with nZVI/AC composites. Potential degradation

products of HCB were monitored. Fig.7 and 8 are trends of various dechlorination by-products (in percentage of initial HCB) against time for nZVI/AC-I and nZVI/AC-A respectively. Intermediates detected include monochlorobenzene (MCB), isomers of dichlorobenzene (DCB), trichlorobenzene (TriCB), tetrachlorobenzene (TeCB) and pentachlorobenzene (PCB). The detection of various intermediates in solution proved that reductive dechlorination reaction by loss of chloride atoms occurred with nZVI/activated carbon. Concentrations of by-products in solution with activated carbon were below detection limit which may indicate that dechlorination by activated carbon was negligible.

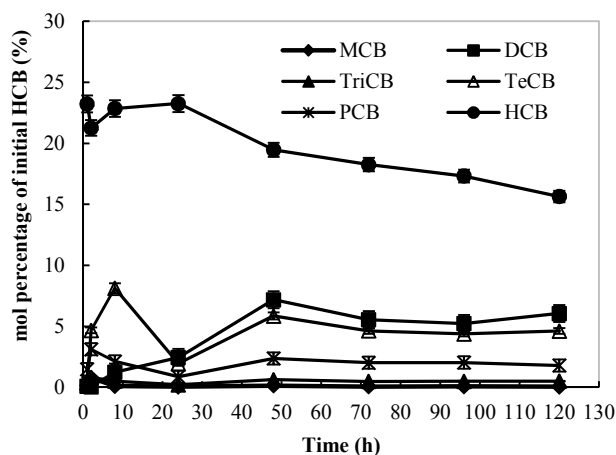


Fig.7 Changes of HCB and its dechlorination by-products vs. time with nZVI/AC-I in solution

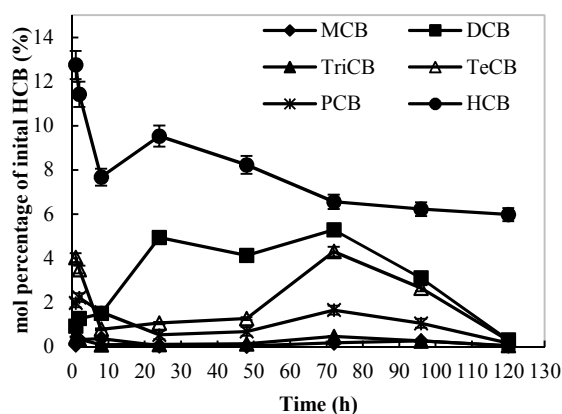


Fig.8 Change of HCB and its dechlorination by-products vs. time with nZVI/AC-A in solution

Mass balance analysis of chlorinated aromatics based on the amount of by-products detected in solution was poor due to the fact that dechlorination intermediates may be retained on activated carbon surface and not released to solution. On average, after 48 h of contact with nZVI/AC-A and nZVI/AC-I, only 35% and 18% of the initial HCB mass was detected in solution indicating strong adsorption from activated carbon. Among them, about 70-80% is HCB and the rest is composed of various dechlorination by-products. In particular, in the case of nZVI/AC-A, concentrations of the by-products peaked at 72 h of contact, then gradually decrease until almost no by-product was detected in solution after 120 h as shown in Fig.8. Dechlorination by-products was taken up by nZVI/AC-A after long contact. This means that it could provide more complete removal of HCB.

Combining mass from solution with that retained on solids, Fig.9 and 10 show trends of HCB and dechlorination intermediates in total. Mass balance analysis showed that around 90% of the mass was accounted for. The remaining 10% may be strongly adsorbed on activated carbon and was not extractable by n-hexane. According to mass analysis, after 2 h, more than 50% the initial HCB was dechlorinated with nZVI/AC-I. After 72 h, HCB accounted for about 20% of the total mass. nZVI/AC-A was able to dechlorinate more than 70% of HCB after 2 hours and only 9.5% of the initial HCB still existed after 72 h. A greater amount of HCB was dechlorinated with nZVI/AC-A. This may also attributed to nZVI/AC-A's higher iron content.

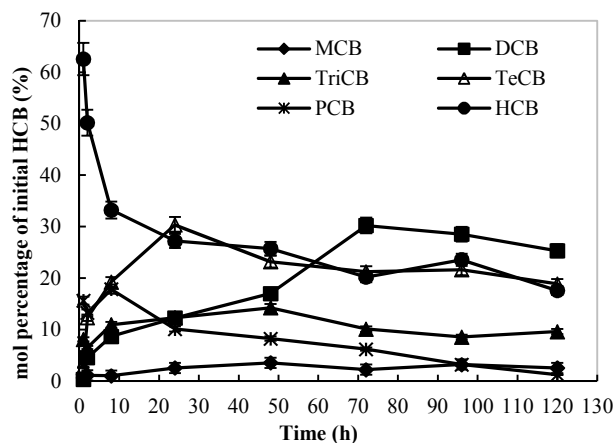


Fig.9 Change of HCB and its dechlorination by-products vs. time with nZVI/AC-I in total

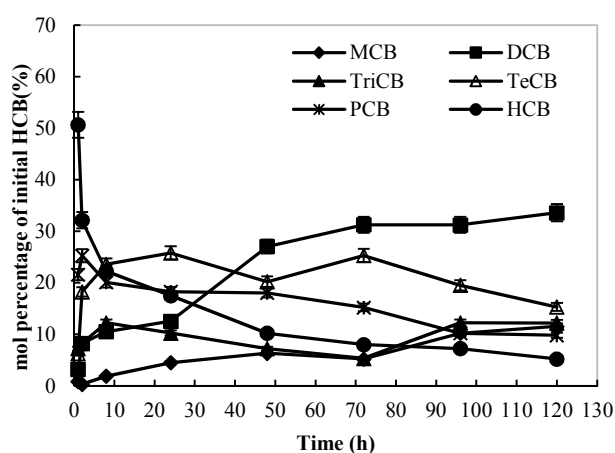


Fig.10 Change of HCB and its dechlorination by-products vs. time with nZVI/AC-A in total

It is generally believed that higher chlorination tended to higher toxicity [32]. Dechlorination by-products are generally less toxic and more biodegradable. Dechlorination showed by both nZVI/AC composites suggests that these products can be used for remediation of HCB in environment.

nZVI/AC-I and nZVI/AC-A showed much similarity as far as dechlorination pathway is concerned as shown in Fig.9 and 10. DCB and TeCB were the main byproducts. 1,4-DCB and 1,2,4,5-TeCB were detected to be the main species of TeCB and DCB in this research. 1,4-DCB and 1,2,4,5-TeCB both manifested symmetric structures and are more stable. Studies have shown that chloride atoms at the first and third carbon have lower electron density, and are much more susceptible to nucleophilic

substitution[33]. Nie and Liu also mentioned 1,2,4,5-TeCB being the main byproducts of PCB dechlorination in their study[34]. However, due to the low concentration of TriCB, no distinction among TriCB isomers was made.

Monitoring of dechlorination by-products showed a clear stepwise dechlorination pattern for both nZVI/AC-I and nZVI/AC-A. There was a general decrease in HCB with the increase of contact time. PCB peaked after 2 h of reaction then slowly decreased until the end of the experiment. TeCB became the predominant specie after 10 h and reached apex at around 48 h. TriCB and DCB were both observed after 8 h. DCB replaced TeCB to become the predominant specie after 72 h. It seems that TriCB dechlorination to DCB was fast and accumulation of TriCB did not occur. Therefore, TriCB never dominated and was stable around 10% after 48 h. Also, percentage of MCB was relatively low throughout the whole test meaning that it may took much longer time for HCB to degrade to MCB.

In summary, the dechlorination results agreed well with several studies of HCB reduction by nZVI [35]. All these studies reported stepwise dechlorination. Also, the percentage of less chlorinated by-products (e.g. DCB and MCB) over initial total HCB was higher with nZVI/AC-A than nZVI/AC-I. After 120 h, DCB and MCB accounted for 40% of the HCB with nZVI/AC-A. This number is 25% for nZVI/AC-I. nZVI/AC-A was more effective in dechlorination.

The dechlorination by-products and pathways in the stepwise reductive dechlorination of HCB with nZVI/AC are as follows: The first product was PCB. PCB quickly dechlorinated to form tetrachlorobenzene which includes three isomers. 1,2,4,5-TeCB is found to be the main product. TriCB was the next step and was further converted to 1,4-DCB. There was also a small amount of MCB detected. So the main pathway proposed was HCB→PCB→1,2,4,5-TeCB→TriCB→1,4-DCB→MCB.

4. Conclusions

nZVI/AC particles were prepared by first loading iron salts iron onto activated carbon and then nZVI was synthesized through a chemical reduction. The performance for HCB removal was investigated and compared with activated carbon and nZVI. Iron loading method played a significant role in the morphology of nZVI and extent of iron content. With the help of ethanol, adsorption method was able to produce nZVI with rod-like structure and thus created nZVI/activated carbon composite boasted much higher iron content.

Batch experiments showed that nZVI/AC composite result in the enhancement of HCB removal and resistance against pH change as compared to activate carbon or nZVI alone. In addition, HCB removal by nZVI/AC fits well with second order reaction consumptions.

Dechlorination of HCB was proven to play a significant part in HCB removal. The majority of HCB was dechlorinated and converted into an array of intermediate chlorobenzen products with TeCB and DCB as the predominant species. Especially, nZVI/AC composite with iron adsorption as the starting step showed advantages in both HCB removal efficiency and dechlorination capability. Removal efficiency reached as high as 95% for HCB and 90% of the removed HCB was dechlorinated after 72 h of reaction.

Overall, combining nZVI with activated carbon was able to take advantage of the adsorption capacity of activated carbon and the dechlorination reactivity of nZVI and resultant material showed great promise as a candidate for HCB remediation.

Acknowledgement

This work was supported by Shanghai Natural Science Foundation (14ZR1428900); National Natural Science

Foundation of China (51078233); by Shanghai Committee of Science and Technology (13230502300) and by Tianjin Natural Science Foundation (13JCYBJC18600).

Notes and References

a School of Environment and Architecture, University of Shanghai for Science and Technology, Shanghai 200093, China.

b College of Marine Science and Engineering, School of Tianjin University of Science and Technology, Tianjin 300457, China.

- M. Tong, S. Yuan, *J. Hazard. Mater.*, 2012, **229-230**, 1.
- J.F. Jarrell, A. Gocmen, D. Akyol, R. Brant, *Reprod. Toxicol.*, 2002, **16**, 65.
- X. Ye, J. Jiang, Y. Yang, G. Gao, *Chem. Eng. J.*, 2011, **173**, 415.
- Y.H. Shih, C.Y. Hsu, Y.F. Su, *Sep. Purif. Technol.*, 2011, **76**, 268.
- S. Klimkova, M. Cernik, L. Lacinova, J. Filip, D. Jancik, R. Zboril, *Chemosphere*, 2011, **82**, 1178.
- K.D. Grieger, A. Fjordboge, N.B. Hartmann, E. Eriksson, P.L. Bjerg, A. Baun, *J. Contam. Hydrol.*, 2010, **118**, 165.
- F. He, D. Zhao, C. Paul, *Water Res.*, 2011, **44**, 2360.
- P.J. Dorathi, P.K. Kandasamy, *J. Environ. Sci.*, 2012, **24**, 765.
- H. Kim, H.J. Hong, J. Jung, S.H. Kim, J.W. Wang, *J. Hazard. Mater.*, 2010, **176**, 1038.
- L.B. Hoch, E.J. Mack, B.W. Hydustky, J.M. Hershman, I.M. Skluzacek, T.E. Mallouk, *Environ. Sci. Technol.*, 2008, **42**, 2600.
- S.A. Kim, S. Kamala-Kannan, K.J. Lee, Y.J. Park, P.J. Shea, W.H. Lee, H.M. Kim, B.T. Oh, *Chem. Eng. J.*, 2013, **217**, 54.
- J. Xu, X. Lv, J. Li, Y. Li, L. Shen, H. Zhou, X. Xu, *J. Hazard. Mater.*, 2012, **225-226**, 36.
- M.C. Pereira, F.S. Coelho, C.C. Nascentes, J.D. Fabris, M.H. Araujo, K. Sapag, L.C.A. Oliveira, R.M. Lago, *Chemosphere*, 2010, **81**, 7.
- S. Bleyl, F.D. Kopinke, K. Mackenzie, *Chem. Eng. J.*, 2012, **191**, 588.
- J.J. Zhan, B. Sunkara, J.J. Tang, Y.Q. Wang, J.B. He, G.L. McPherson, V.T. John, *Industr. Eng. Chem. Res.*, 2011, **50**, 13021.
- H.Q. Sun, G.L. Zhou, S.Z. Liu, H.M. Ang, M. O Tade, S.B. Wang, *Appl. Mater. Interface*, 2012, **4**, 6235-6241.
- H.H. Tseng, J.G. Su, C. Liang, *J. Hazard. Mater.*, 2011, **192**, 500-506.
- P. Jiemvarangkul, W. Zhang, H. Lien, *Chem. Eng. J.*, 2011, **170**, 482-491.
- R.D. Rogers, A.H. Bond, C.B. Bauer, *Sep. Sci. Technol.*, 1993, **28**, 139.
- J.T. Jiu, L.P. Li, Y. Ge, S.R. Zhang, Z.R. Hua, L. Nie, *Chinese J. Inorg. Chem.*, 2001, **17**, 361.
- M. Mohapatra, H. Mohapatra, P. Singh, S. Anand, B.K. Mishra, *Int. J. Eng. Sci. Technol.*, 2010, **2**, 89-103.
- V.I. Protilla, *Am. Mineral.*, 1976, **61**, 95.
- A.L. Andrade, D.M. Souza, M.C. Pereira, J.D. Fabris, R.Z. Domingues, *Ceramica.*, 2009, **55**, 420.
- G. Roy, P.D. de Donato, T. Görner, O. Barres, *Water Res.*, 2003, **37**, 4954.
- M.L. Godino-Salido, R. López-Garzón, M.D. Gutiérrez-Valero, P. Arranz-Mascarós, M. Melguizo-Guijarro, M. D. L. de la Torre, V. Gómez-Serrano, M. Alexandre-Franco, D. Lozano-Castelló, D. Cazorla-Amorós, M. Domingo-García, *Mater. Chem. Physic.*, 2014, **143**, 1489.
- S. Yuan, Z. Zheng, X.Z. Meng, J. Chen, L. Wang, *Geoerma*, 2010, **159**, 165.
- Y.H. Shih, Y.C. Chen, M.Y. Chen, Y.T. Tai, C.P. Tso, *Colloid Surf. A: Physicochem. Eng. Asp.*, 2009, **332**, 84-89.
- N. Zhu, H. Luan, S. Yuan, J. Chen, X. Wu, L. Wang, *J. Hazard. Mater.*, 2010, **76**, 1101.

-
- 29 X. Xu, J. Wo, J. Zhang, Y. Wu, Y. Liu, *Desalination*, 2009, **242**, 346.
30 X. Nie, J. Liu, X. Zeng, D. Yue, *J. Environ. Sci.*, 2013, **25**, 473.
31 Deng, D.R. Burniss, T.J. Campbell, *Environ. Sci. Technol.*, 1999, **33**,
2651.
5 32 A. Poland, J.C. Knutson, *Annu. Rev. Pharmacol. Toxicol.*, 1982, **22**,
517.
33 Y. Xu, W.X. Zhang, *Ind. Eng. Chem. Res.*, 2000, **39**, 2238.
34 X. Nie, J.G. Liu, *J. Environ. Sci.*, 2013, **25**, 473-478.
35 G.V. Lowry, K.M. Johnson, *Environ. Sci. Technol.*, 2004, **38**, 5208.

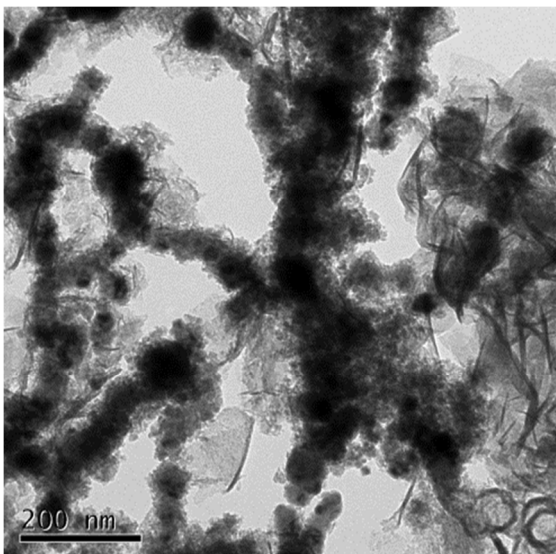
10

15

20

Table of content:

1. Color graphic



2. Novelty of the work:

HCB was removed by nano ZVI/AC composite by both adsorption and dechlorination. Dechlorination was stepwise and pathway proposed.